Full Characterization of Water Transport Properties in Polyetherketoneketone (PEKK)

Gwladys Lesimple, Ilias Iliopoulos, Jean-Baptiste Marijon, Bruno Fayolle

Full characterization of water transport properties in polyetherketoneketone (PEKK)

Gwladys LESIMPLE[1], Ilias ILIOPOULOS[1], Jean-Baptiste MARIJON[1], Bruno FAYOLLE[1]*

[1]*Laboratoire PIMM, Arts et Metiers Institute of Technology, CNRS, Cnam, HESAM Universite, 151 boulevard de l'Hopital, 75013 Paris (France)*

Abstract

Polyetherketoneketone (PEKK) is of increasing interest for the manufacture of composites in the aeronautical field. It is essential to evaluate PEKK absorption of fluids, especially water, with which it may come into contact during its processing and use. In this work, we provide for the first time water transport parameters such as water diffusivity and solubility for PEKK in amorphous and semicrystalline states using water immersion as well as Dynamic Vapor Sorption (DVS) experiments. Water diffusion is modelled using Fick's second law with variable boundary conditions, taking into account possible relative humidity variation during the DVS experiments. Based on similar characterizations on PEEK (polyetheretherketone), we discuss the fact that PEKK absorbs more water than PEEK in terms of polarity.

Keywords: PEKK, water, diffusion, solubility, DVS

*Corresponding author: bruno.fayolle@ensam.eu; Laboratoire PIMM, Arts et Metiers Institute of Technology, CNRS, Cnam, HESAM Universite, 151 boulevard de l'Hopital, 75013 Paris (France)

1. Introduction

High performance thermoplastics are gaining in interest the last decades particularly in the aeronautical field. These thermoplastics aim to replace thermoset matrices currently used in structural composite parts of aircrafts [1,2]. The most used include the amorphous polymer polyether imide (PEI) and the semicrystalline polyaryletherketones (PAEK) and polyphenylene sulfide (PPS) [3]. PAEK family seems to be the best candidate as it allows higher in-service temperature than PPS (T_g (PAEK) ≈ 132-187°C vs T_g (PPS) ≈ 85-95°C) and has a good oxidative and fire resistance owing to its aromatic chain [4–8]. Polyetherketoneketone (PEKK) has been recently industrialized to complete the range of PAEK polymers as a matrix in carbon fiber reinforced composite parts in the aerospace industry (Figure 1). PEKK is comparable with PEEK regarding mechanical performance, thermal and chemical resistance but presents the advantage of having a tunable melting temperature when changing the ratio of T and I units along the chain. Indeed, PEKK is made of both terephtaloyl isomer (T) with *para* phenyl links and isophtaloyl isomer (I) with *meta* phenyl links, leading to two kinds of dyads: TT or TI [6,9]. The more isophtaloyl isomer in the copolymer, the lower the melting temperature: T_m = 300-360°C for T/I ratio varying from 60/40 to 80/20) [4,10,11]. PEKK with T/I = 70/30 (T_g = 162°C, T_m = 332°C) is specifically designed for composites [12]. It has a higher T_g and a lower T_m as compared to PEEK (T_g = 143°C and T_m = 343°C) offering a combination of higher in-service temperature and easier processing conditions [13].

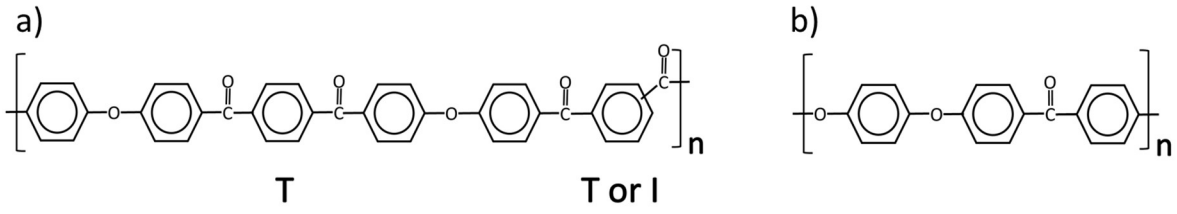

Figure 1 Chemical structure of PEKK constituted of TT and TI dyads (a) and PEEK (b)

The presence of water in the polymer matrix can affect the mechanical properties of the composite parts [14,15]. Indeed, during its use, the composite behavior can be affected by the presence of water because of the plasticization of the matrix [16]. Moreover, during the manufacturing of the composite parts, when the processing temperature exceeds T_g, the water contained in the matrix goes to the gaseous state, which can induce a porosity as well as a debonding at the interface between the carbon fibers and the polymer matrix [17–20]. For these reasons, quantity of absorbed water and water transport mechanism in polymer matrices should be assessed as a function of exposure conditions. This assessment should provide diffusivity and solubility parameters of water to simulate these processes into polymer matrix of industrial parts.

If water transport in PEEK is fully detailed in literature, no information is available about water transport in PEKK. For instance, a first study by Stober *et al.* in 1984 [21] indicates a great resistance of PEEK to water in terms of chemical ageing such as hydrolysis. More recently, water sorption mechanism has been studied in neat PEEK resin by immersion and the use of environmental chambers controlled in temperature and relative humidity (RH) [22]. Concerning the PEKK, one can note that most of the studies on PEKK resin are devoted to crystallization kinetics and mechanical behavior in relation to crystal morphology [2],[6],[14]. To our knowledge, no paper reports on the sorption of water in neat PEKK and only few studies provide data on the sorption of water by composites consisting of carbon fiber reinforced PEKK [24,25].

This paper aims to provide first data for water sorption in PEKK resin at different relative humidities and temperatures. These data are compared to those of PEEK by performing the same experiments on the latter. Knowing that these polymers will be used in semicrystalline form in the case of carbon fiber reinforced composites, water transport in amorphous and semicrystalline states is investigated in various relative humidity conditions and in immersion as well.

2. Experimental

2.1. Materials

The experiments are performed using commercially available PEKK (T/I ratio of 70/30) commercialized under trademark Kepstan® 7002 as well as PEEK commercialized under trademark Victrex™ PEEK 450G. PEKK and PEEK are both provided as amorphous films and in the form of 2 mm-thick (100x100 mm²) injected plates. The films are extruded at 347°C (PEKK) and 370°C (PEEK) and the plates are injected at 355°C (PEKK) and 380°C (PEEK). PEKK films are 50, 150 and 250 µm-thick whereas PEEK film is 50 µm-thick. Crystalline samples are obtained by annealing at 200°C (see next section). To assess samples crystallinity, Wide Angle X-ray Scattering (WAXS) measurements are performed on both crystallized 50 µm-thick films and crystallized 2 mm-thick injected PEKK and PEEK plates (Table 1). WAXS spectra analysis is done as previously reported by Tencé-Girault et al. for PEKK 6002 [26]. The WAXS spectra of the amorphous films show no peak linked to a crystalline phase, only broad peaks corresponding to the amorphous phase. SAXS results confirm this fully amorphous state. The data are very similar to those reported by Tencé-Girault et al. for PEKK 6002 [26].

Table 1
Weight crystallinity measured by WAXS in the crystallized PEKK and PEEK films and plates

	PEKK		PEEK	
	50 µm film	**2 mm plate**	**50 µm film**	**2 mm plate**
X_c (%)	15	19	23	22

Gravimetric measurements are performed on the 2 mm-thick plates while thin films are used for dynamic vapor sorption (DVS) measurements.

2.2. Gravimetric measurement

Samples of size 50x50 mm² are cut using a band saw in the 2 mm-thick injected plates (PEKK and PEEK). Then, the edges are sanded with sandpaper in order to smoothen the surfaces. Prior to the immersion in water, the specimens are first dried in a vacuum oven at 20 mbars (with no dynamic control of the

vacuum level) at 120°C during 48 hours. Then, the plates are annealed at 200°C for 4 hours in a classical oven in order to control the crystallinity of the polymers. The cooling rate is not controlled; the oven is switched off and the samples are cooled down until 80°C (well below the T_g for both PEKK and PEEK) before removing them from the oven. PEKK and PEEK samples are immerged in distilled water in glass jars closed with a rubber seal. The jars are placed in a temperature-regulated water bath at 30°C, 50°C and 70°C. The samples are regularly surface-dried with paper towel and weighed using a Mettler Toledo analytical balance. The experimental data points are averaged over five samples. The masses obtained are converted into mass percentage of absorbed water (*w*) using the following equation:

$$w = \frac{m - m_0}{m_0} \times 100 \quad (1)$$

With *m* the mass of the sample at time *t* and m_0 the initial mass of the dried sample.

Once saturated, the samples are placed in a vacuum oven at 120°C in order to desorb water and verify the reversibility of the water absorption. The samples are weighed until a stable mass is reached. No gravimetric data are available for amorphous PEKK and PEEK as it was not possible to obtain amorphous 2 mm-thick plates by injection molding because of the high crystallization rate of both polymers.

As a complement, five typical gravimetric PEKK samples (50x50x2 mm^3) are exposed in a room controlled in temperature and relative humidity (23°C/64% RH). The samples are weighed regularly until saturation in order to compare with DVS results.

2.3. Dynamic Vapor Sorption

Water vapor sorption experiments are performed at different relative humidities using IGAsorp Dynamic Vapor Sorption (DVS) apparatus from Hiden Isochema. Samples of dimensions 30x15 mm^2 are cut from the 50 µm-thick films. Some complementary experiments are carried out using 150 µm-

thick and 250 µm-thick amorphous PEKK films (see Supplementary Information). The DVS apparatus is set to record the sample mass, relative humidity and temperature every 25 seconds.

Semicrystalline samples are obtained by annealing the amorphous films in an oven during 4 hours at 200°C. No other specific treatment has been performed. We will assume that the ketone concentration is the same at the film surface than in the bulk. The amorphous samples are not conditioned before experiment. Each sample is perforated in the top part and suspended by a hook in the DVS chamber regulated in temperature, linked to a microbalance of resolution 0.05 µg. The relative humidity is controlled throughout the experiment by a mix of a dry 100 mL/min nitrogen flow and a humidified flow (coming from a water bath controlled in temperature) using mass flow controllers[27]. Each isothermal experimentation is performed with a relative humidity cycle imposed as follows: 0% RH - 10% RH - 0% RH - 30% RH - 0% RH - 50% RH - 0% RH - 70% RH - 0% RH - 90% RH - 0% RH. The RH-plateau duration is the same for the whole cycle and depends on the polymer and the temperature. Each experiment is repeated at least twice on different samples in order to verify the repeatability of the test (see Section 1 in Supplementary Information).

2.4. Water diffusion model

Gravimetric measurement data obtained by immersion and in humid air are analyzed in order to plot the mass percentage of absorbed water as a function of time. The quantity of water absorbed at saturation (w_∞) is determined for different temperatures as:

$$w_\infty = \frac{m_\infty - m_0}{m_0} \times 100 \quad (2)$$

With m_∞ the sample mass at saturation and m_0 the initial mass of the dried sample. This holds whatever we are in immersion or at different RH conditions.

The diffusion coefficient is defined by Fick's second law:

$$\boldsymbol{J} = -D\nabla w \quad (3)$$

With *J* the diffusion flux vector and *D* the diffusion coefficient of water in the polymer.

A numerical resolution is implemented in order to determine the diffusion coefficient by taking into account the weight gain measured during the entire experiment. Considering a 1D problem, Fick's law is simplified as follows:

$$\frac{dw}{dt} = D\frac{\partial^2 w}{\partial x^2} \tag{4}$$

The water uptake *w* is discretized both in time (*t*) and space (*i*) in the 1D sample of thickness *h*:

$$\frac{dw(t,i)}{dt} = \frac{D}{dx^2}\big(w(t,i+1) - 2w(t,i) + w(t,i-1)\big) \tag{5}$$

With *w(t,i)* the water mass percentage at time *t* in layer *i*.

The water mass percentage at the sample surface is equal to the mass percentage of water absorbed at saturation for a specific value of relative humidity. For the numerical modeling, two hypotheses are considered at the initial state:

i. the bulk sample is considered dry at *t = 0*,
ii. the relative humidity is considered constant on the surfaces of the sample of thickness *h* during the entire experiment, thus, w_∞ is constant at the sample surfaces.

The initial and boundary conditions can be written as:

$$\begin{cases} w(0,i) = 0, & t = 0, 0 < i < h \\ w(t,0) = w(t,h) = w_\infty, & t \geq 0 \end{cases} \tag{6}$$

The second hypothesis leads to the following condition on the derivative at the sample surfaces (*i = 0* and *i = h*):

$$\frac{dw(t,0)}{dt} = \frac{dw(t,h)}{dt} = 0 \tag{7}$$

A MATLAB Ordinary Differential Equation (ODE) solver is used to solve Fick's differential equation (eq. 4). The diffusion coefficient is determined by the finite difference method in order to obtain an optimized value based on all the experimental data points. Two variables *tspan* and *hspan* are implemented to set the time step (number of divisions of the total time) and the space step (number of divisions of the thickness *h*). The two parameters *tspan* and *hspan* are set to 50 and 100 in the present study. First, an initial value for *D* is implemented, the numerical resolution starts solving the system. The average water uptake *w* is calculated at each time and subtracted to the experimental data. The value for *D* is updated and the process is repeated until the gap between the experimental data and the model is satisfactory (tolerance set to 10^{-13}).

For DVS data, it is necessary to take into account the relative humidity recorded during the experiment (see Supplementary Information). Therefore, the water mass percentage at the sample surfaces is now considered a linear function of RH. The water uptake at saturation (w_∞) at both surfaces is not constant anymore. As the relative humidity takes several minutes to reach the set value, w_∞ varies with time during this transition step from 0% to the set plateau value. It depends on the real value of relative humidity measured experimentally at time *t*. The boundary conditions from equation 6 now change for every time step such that:

$$\begin{cases} w(0,i) = 0, & t = 0, 0 < i < h \\ w(t,0) = w(t,h) = w_\infty(t), & t \geq 0 \end{cases} \quad (8)$$

These boundary conditions are implemented in the new MATLAB program in order to take into account the progressive increase of relative humidity at short times.

3. Results

The gravimetric measurements in liquid water are done on thick plates of crystalline PEKK and crystalline PEEK (2 mm). Indeed, it was not possible to manufacture amorphous thick plates. The DVS measurements (at different relative humidities) are done on thin films (50 µm for most of them) of

both amorphous and crystalline PEKK and PEEK. The gravimetric measurements by immersion of thin films in liquid water were not possible as the films are too light to have relevant gravimetric measurements. The use of thick plates provides more reproducible results in this case.

3.1. Water immersion of crystalline PEEK and PEKK

Water immersion is the most common experimental method for obtaining an estimate of the diffusion coefficient of water for a given polymer. Here, water immersion is performed on crystallized PEKK and PEEK plates at 30°C, 50°C and 70°C. Weight gain as a function of reduced time (square root of time normalized by the thickness) is presented in Figure 2. The results are presented with error bars in Supporting Information Figure S1. First, we can note that weight gain values after saturation are lower than 1%. Compared to thermosets, these values are low knowing that low T_g epoxy resins can absorb up to 5 % after saturation in water due to the strong interactions between water molecules and epoxy resin structural units [28–31].

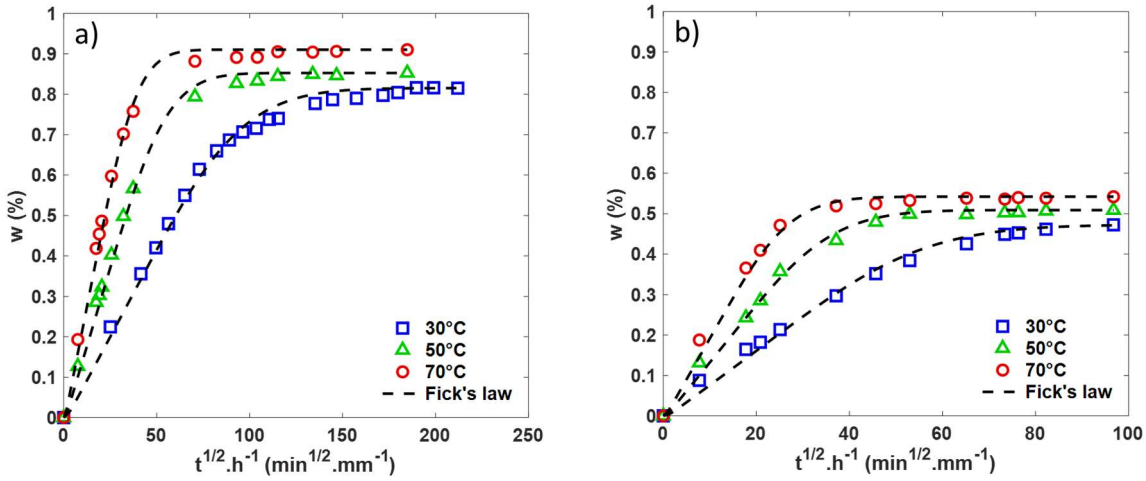

Figure 2 Weight gain in immersion, at three temperatures (30°C, 50°C and 70°C), as a function of reduced time for crystallized PEKK (a) and PEEK (b). Data are fitted with Fick's law (dotted line) for each condition.

The weight gain as a function of reduced time shows an initial linear part, which is typical of fickian behavior. Since the modeling by Fick's law using the MATLAB solving describes very well the data (see dotted line for each condition of exposure), diffusion coefficients obtained with constant boundary conditions as well as the total weight gains are reported in Table 2. Despite the low number of data

points at short times for PEEK immersed at 70°C, the numerical model allows a satisfactory determination of the diffusion coefficient.

Table 2
Diffusion coefficient and weight gain at saturation for crystallized PEKK and PEEK measured by water immersion at 30°C, 50°C and 70°C

	PEKK		PEEK	
T (°C)	**$Dx10^{12}$ ($m^2.s^{-1}$)**	**w_∞ (%)**	**$D\ x10^{12}$ ($m^2.s^{-1}$)**	**w_∞ (%)**
30°C	0.4 ± 0.1	0.82 ± 0.02	1.0 ± 0.1	0.48 ± 0.01
50°C	1.1 ± 0.1	0.85 ± 0.01	2.5 ± 0.2	0.51 ± 0.01
70°C	2.2 ± 0.2	0.91 ± 0.01	4.9 ± 0.3	0.54 ± 0.01

The standard deviation of *D* is obtained by finding upper and lower bounds of the experimental data by implementing different diffusion coefficients in the numerical program. This method leads to minimum and maximum values of the diffusion coefficient. Concerning standard deviation of w_∞, it is calculated with the weight gains of the different samples as described in Section 2.

From the data in Table 2, it appears the diffusion coefficient increases with temperature following Arrhenius behavior with an activation energy of 40 $kJ.mol^{-1}$ and 37 $kJ.mol^{-1}$ for PEKK and PEEK respectively. A slight variation of the weight gain at saturation with the temperature is observed for both polymers with an activation energy of 2.2 $kJ.mol^{-1}$ and 2.5 $kJ.mol^{-1}$ for crystallized PEKK and PEEK respectively. The initial mass (m_0) of the samples is recovered after drying at 120°C under vacuum, showing that water sorption is a fully reversible mechanism in both PEKK and PEEK. This indicates that no damage, such as hydrolysis, occurs in the polymers during water immersion. The differences observed between PEKK and PEEK will be discussed in Section 4.

3.2. Influence of the relative humidity and temperature

The influence of the relative humidity and temperature on water transport parameters for PEKK and PEEK is presented in this section. To study water sorption as a function of humidity and temperature, Dynamic Vapor Sorption (DVS) is the most appropriate technique. DVS was developed in the 90s to

replace the traditional gravimetric methods, e.g. environmental chambers and saturated salt solutions, which are very laborious, time-consuming and, to some extent, operator dependent [32]. DVS is an automated device used to measure water uptake and diffusion at different relative humidities in short times with high accuracy. It has been widely used in the food industry, usually on powder samples [33–35] as well as for wood materials [27,32]. Few studies demonstrate the suitability of DVS for polymer resins [36,37].

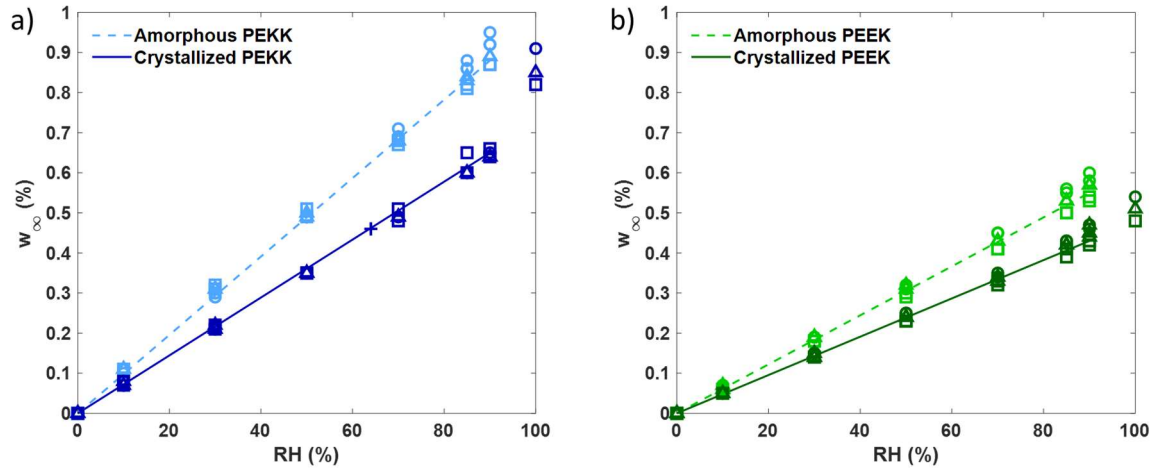

Figure 3 Weight gain at saturation as a function of relative humidity for amorphous and crystallized PEKK (a) and PEEK (b) at 30°C (□), 50°C (△), 70°C (○) and 23°C/64% RH (+). Data are fitted with a linear relationship according to Henry's law (dashed line for amorphous samples and solid line for crystallized samples).

Figure 3 reports the equilibrium weight gain for several relative humidities and temperatures for all polymers studied. The saturation weight gain clearly increases with relative humidity (RH). The linear relationship between water uptake and relative humidity between 0% and 90% RH shows that PEKK and PEEK (both amorphous and crystalline) follow Henry's law in this RH range. In other words, water concentration at equilibrium C_∞ calculated from w_∞ is directly proportional to the water vapor pressure (p_w) associated to RH as following:

$$\frac{w_\infty \rho_p}{M_{water}} = C_\infty = S p_w \quad (9)$$

With p_w the water vapor pressure, S solubility of water into the polymer, ρ_p the polymer density and M_{water} the molar mass of water. The solubility as well as its activation energy H_S (*i.e.* water heat of dissolution) are indicated in

Table **3**. As the relative humidity (*RH*) is the ratio of the vapor pressure of water (p_w) to the saturation water vapor pressure (p_{sat}), the mass percentage of absorbed water can be written as:

$$w_\infty = K_H \frac{RH}{100} \tag{10}$$

With K_H the Henry's law solubility constant (see

Table **3**).

Finally, the solubility (S) is calculated using the following equation:

$$S = \frac{100 w_\infty \rho_p}{M_{water} RH p_{sat}(T)} \tag{11}$$

Table 3
Diffusion (D) and solubility (S) parameters (at 50°C), activation energies (E_D for diffusion and H_S for solubility) of water in PEKK and PEEK measured by DVS at 70%HR and Henry parameter (K_H)

	χ_c (%)	D at 50°C ($m^2.s^{-1}$)	E_D ($kJ.mol^{-1}$)	S at 50°C ($mol.cm^{-3}.Pa^{-1}$)	$\lvert H_S \rvert$ ($kJ.mol^{-1}$)	K_H
PEKK	amorphous	$(1.9 \pm 0.1)\times10^{-12}$	42	$(5.9 \pm 0.3)\times10^{-9}$	43	0.98
	15%	$(1.0 \pm 0.1)\times10^{-12}$	50	$(4.2 \pm 0.3)\times10^{-9}$	43	0.71
PEEK	amorphous	$(2.8 \pm 0.2)\times10^{-12}$	45	$(3.7 \pm 0.2)\times10^{-9}$	41	0.61
	23%	$(2.0 \pm 0.1)\times10^{-12}$	53	$(2.9 \pm 0.1)\times10^{-9}$	42	0.48

The weight gain at saturation does not depend on temperature at low relative humidities (RH < 70%) but slightly increases with temperature at RH > 70% (Figure 3). The water immersion results confirm this small increase of w_∞ with temperature (Table 2). Therefore, the weight uptake at saturation is potentially more temperature dependent at higher relative humidities. To check this point, we report in Figure 4 the experimental data of w_∞ available in the literature as a function of temperature in Arrhenius plots. These data are only for the weight gain at saturation for PEEK in the case of water

immersion [38]. For each set of data coming from the same reference, we have assessed the activation energy E_W (values are indicated in Figure 4). Excepted values from Courvoisier et al., it appears that water concentration increases slightly with temperature in PEEK, which is consistent with the trend observed here for the PEKK.

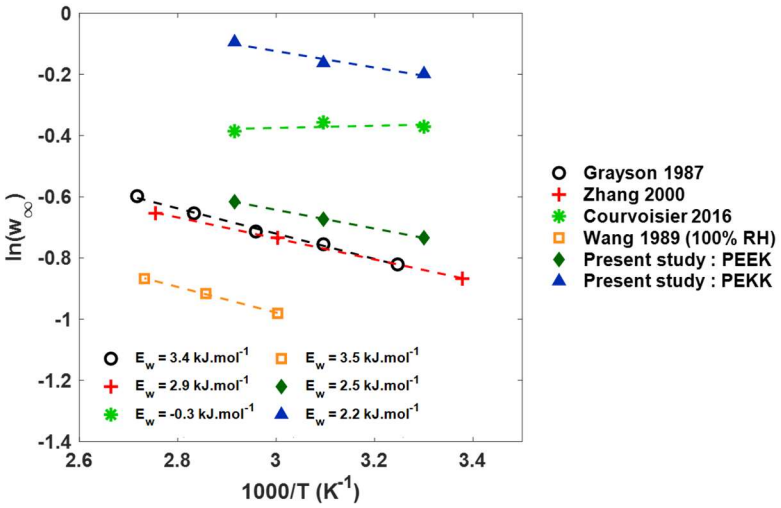

Figure 4 Arrhenius plot of weight gain at saturation from literature for crystallized PEEK water immersion and present study's values for crystallized PEKK and PEEK

The resulting activation energy computed for immersion of crystallized PEEK between 30°C and 70°C is E_w = 2.5 kJ.mol^{-1} (E_w = 3.4 kJ.mol^{-1} according to Grayson and Wolf in the range of 35°C to 95°C). It is worth noticing that the crystallinity measured by DSC for the different literature samples are in the range of 30 to 40%, which can explain a small variation among the results. This small activation energy value can be explained from the fact that the absolute value of the water heat of dissolution H_S (see Table **3**) is close to the heat of water vaporization H_V (H_V = 43 kJ.mol^{-1}) for relatively low polarity polymers like PAEKs [8]. Indeed, equilibrium water concentration can be expressed as follows:

$$C_\infty = C_0 \exp\left(\frac{-H_C}{RT}\right) \; with \; C_0 = S_0 p_0 \; and \; H_C = H_S + H_V \qquad (12)$$

With C_∞ the water concentration, H_C the activation energy of the concentration and C_0, S_0 and p_0 constants [39].

According to equations (9) and (12), C_∞ hardly depends on the temperature which is consistent with the average value of 3 kJ.mol^{-1} measured in Figure 4.

The reduction in water sorption in semicrystalline PEEK compared to the amorphous state (ca. -21%) corresponds to the weight degree of crystallinity (χ_c = 23%) which is considered impermeable to water as often observed for semi-crystalline polymers [29,40]. In the case of semicrystalline PEKK, it appears that crystallinity (X_c = 19%) has a much stronger effect on the water transport properties (w_∞ decreases by 28% for PEKK). One can propose that semicrystalline PEKK has a dense amorphous structure, such as rigid amorphous fraction [41], that limits water absorption and diffusion.

4. Discussion

4.1. Diffusion coefficient values

In Figure 5, we report literature data of water diffusion coefficient measured by water immersion of crystallized PEEK. If a similar trend for all sets of data can be observed, with activation energy values between 34 and 43 kJ.mol^{-1}, one can note that Wang et al. give results obtained at 100% RH, which differ from complete immersion, and shows an activation energy close to 22 kJ.mol^{-1} [42]. According to this observation, we propose to check if the activation energy for the diffusion can be impacted by the relative humidity.

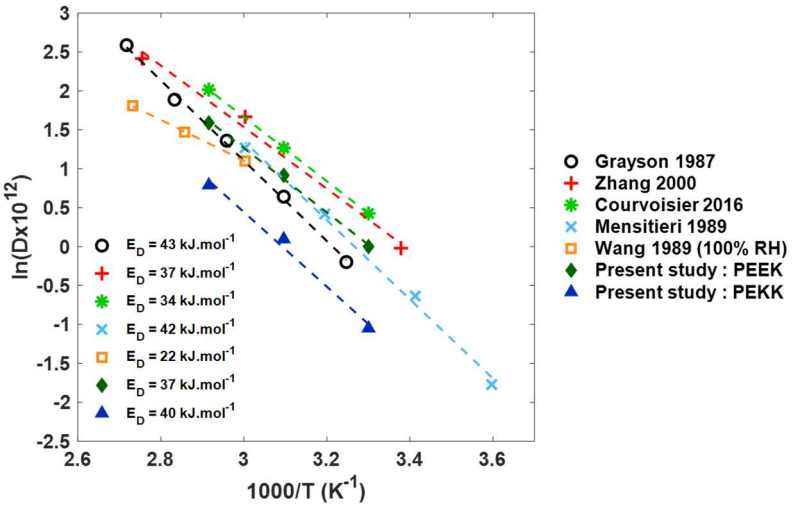

Figure 5 Arrhenius plot of diffusion coefficients from literature for crystallized PEEK water immersion and present study's values for crystallized PEKK and PEEK [22,29,38,42,43]

The Arrhenius plot of the diffusion coefficient measured by DVS at 70% RH, for both amorphous and crystalline PEKK and PEEK, is presented in Figure 6. The graph shows data of each experiment, which is repeated two to three times for each temperature. We remind that, in this RH range, the diffusion coefficient measured by DVS is independent of film thickness and RH (see Figure 4 in Supplementary Information). Similar values of E_D are found for both PEKK and PEEK which may be attributed to the similarities in their chemical structure (Figure 1) and to the fact that the experiments were performed in a temperature range (30°C-70°C) well below their T_g's (respectively 143°C and 162°C for PEEK and PEKK).

Interestingly, the activation energy measured by DVS is slightly higher than the one measured by water immersion. This may be related to the tendency of sur-saturation of the polymer by water during immersion experiments, facilitating water diffusion when increasing temperature. However, we note that the E_D values extracted from the immersion experiments remain in the range of activation energies found in literature (see Figure 5) [22,29,38,42,43].

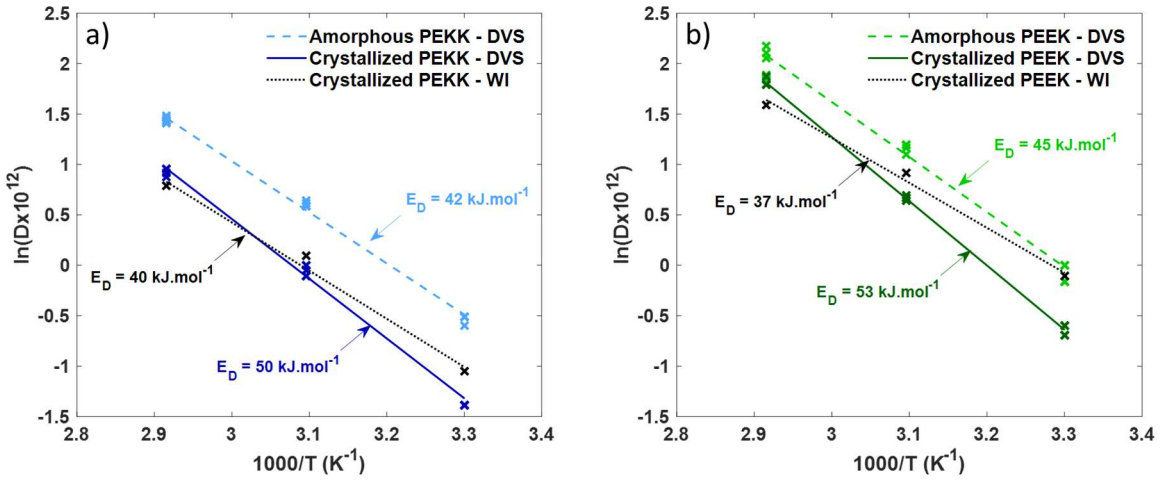

Figure 6 Arrhenius plots of the diffusion coefficient for amorphous and crystallized PEKK (a) and PEEK (b) measured by DVS at 70% RH and water immersion (WI)

4.2. Influence of the polymer polarity

To highlight the effect of polymer polarity on the water transport parameters, w_∞ and D, we consider here the PEKK and PEEK polymers in the amorphous state. The comparison of crystalline samples is complex because it is difficult to obtain PEKK and PEEK samples with the same crystallinity content.

Our results, for the amorphous samples, show that water diffusion is slower in PEKK than in PEEK (Table 2,

Table 3, Figure 6). According to Carter and Kibler [44], water molecules are present in two states in the polymer: free water and bound water. The latter is linked to polar sites present in the polymer and is dynamically released becoming free water with a diffusion coefficient D. As PEKK contains twice as many ketone groups as PEEK, knowing that the latter has a ketone/ether ratio of 67% against 33% for PEEK, the number of polar sites is twice as high. This high number of polar sites leads the water molecules to bind more frequently, thus slowing down the diffusion in the amorphous sample by a ratio of 1/3 (

Table **3**). A FTIR study would be interesting to quantify the ratio between bound and free water in PEKK and PEEK. Nevertheless, it is out of the scope of this study [45,46].

On the other hand, in a first approach, the fact that PEKK absorbs more water than PEEK for the same relative humidity/temperature combination can be discussed through the solubility parameter (δ) [47]. This parameter is directly linked to the chemical structure (i.e. the quantity of polar groups) of both solvent and polymer. Hildebrand [47] defines the total solubility parameter as follows:

$$\delta = \left(\frac{E_{coh}}{V}\right)^{\frac{1}{2}} \tag{13}$$

With δ in $MPa^{1/2}$, E_{coh}, the cohesive energy, in joules and V the molar volume in cm^3. Small [48] rewrites the cohesive energy as a function of the molar attraction constants and the molar volumes of the chemical groups:

$$E_{coh} = \frac{(\sum F_i)^2}{\sum V_i} = \frac{F}{V} \tag{14}$$

With F_i the molar contribution and V_i the molar volume of chemical group i. The solubility parameter's expression becomes:

$$\delta = \frac{\sum F_i}{\sum V_i} \tag{15}$$

Several values for the molar contribution of chemical groups found in literature are gathered by van Krevelen [47]. In the present study, three values of molar contributions are averaged for the calculation of the solubility parameters of PEKK and PEEK (Table 4).

Table 4
Molar contribution (F) and molar volume (V) of phenyl (-Ph), ketone (-CO-) and ether (-O-) groups [47–49]

	F (Small) [48]	F (van Krevelen) [47]	F (Hoy) [47]	F (average)	V (Fedors) [49]	δ_{PEKK}	δ_{PEEK}
		$J^{1/2}.cm^{3/2}.mol^{-1}$			$cm^3.mol^{-1}$	$MPa^{1/2}$	
-Ph	1504	1517	1398.4	1473.1	71.4	24.3	23.4

-CO-	563	685	538.1	595.4	10.8
-O-	143	256	235.3	211.4	3.8

The closer the solubility parameters of the fluid and of the polymer, the more the polymer has affinity for the solvent [5,50]. In the present case, the fluid considered is water, having a solubility parameter of 47.8 $MPa^{1/2}$ [51]. According to equation 15, the solubility parameters for PEKK and PEEK are close (although somewhat higher for PEKK, see Table 4) and cannot explain the experimentally observed differences in water affinity for PEKK and PEEK. Another method includes the Hansen's three-parameter solubility parameter such that [51]:

$$\delta_t{}^2 = \delta_d{}^2 + \delta_p{}^2 + \delta_h{}^2 \qquad (16)$$

With δ_t the total (or Hildebrand) solubility parameter, δ_d the dispersion solubility parameter, δ_p the polar solubility parameter and δ_h the hydrogen bonding solubility parameter.

The three solubility parameters and the total solubility parameters for PEKK and PEEK are given in Table 5.

Table 5

Hansen's solubility parameters and Hildebrand total solubility parameters for PEKK and PEEK [51,52]

	δ_d	δ_p	δ_h	δ_t
		$J^{1/2}.cm^{3/2}.mol^{-1}$		
PEKK	22.1	7.2	3.1	23.45
PEEK	21.4	5.7	3.3	22.39

As for the solubility parameters calculated with equation 13, the Hildebrand solubility parameters for PEKK and PEEK are very close.

Nevertheless, the difference in water affinity could be explained by the greater dipolar moment of ketone group compared to ether group [53]. In addition, the distance between polar groups may play a role in the hydrogen bonding between the water molecules and the polymer matrix. According to

Gaudichet-Maurin et al., a polar site could be composed of one water molecule for two neighboring polar groups instead of one [54]. In that case, the distance between the two polar sites is decisive for the double hydrogen bonding to form. If the water molecules are doubly bonded to polar sites, the solubility of water in PAEK is expected to increase with the ketone concentration in the polymer. This could explain the increased solubility in PEKK compared to PEEK. It is of interest to note that Coulson et al. [55] evidenced the interaction between ketone and water molecules by dynamic mechanical analysis as a gamma relaxation at low temperature ($T_\gamma \approx -96°C$) in PEKK and PEEK. This relaxation mode disappears when the polymers are in a dehydrated state.

Conclusions

Water transport is studied in PEKK in the range of 30-70°C at different relative humidities using water immersion and dynamic vapor sorption (DVS) and compared to PEEK. Compared to data obtained in immersion, DVS is proven to be a fast and reliable method for measuring diffusion coefficient and solubility providing that the assessment is based on Fick's second law with variable boundary conditions. Thus, the water diffusion coefficient for PEKK in amorphous and semicrystalline states could be determined accurately in the 30°C-70°C range. Based on the DVS measurements, water uptake in PEKK is found to follow Henry's law as for PEEK between 0 and 90% RH. To the best of our knowledge, this is the first study offering a full set of data of water solubility in PEKK.

Based on our PEKK and PEEK data and an exhaustive compilation of data available for the latter, this study sheds light on the effect of chemical structure on water transport. Here, PEKK absorbs more water than PEEK but diffusion is slower presumably because water molecules bind to polar sites (i.e. ketones) that are more numerous in PEKK.

Supporting Information

Experiments assessing reproducibility of gravimetric measurements; Comparison of DVS results using models to determine water transport parameters (w_∞ and D) with constant and variable boundary conditions.

Acknowledgement

This work was conducted under the framework of HAICoPAS, a PSPC project (projet de recherche et développement structurant pour la compétitivité). BPI France is acknowledged for funding the PhD work of G. Lesimple (project number: PSPC.AAP-7.0_HAICoPAS). The authors thank Arkema, Hexcel for providing materials and the Industrial Chair Arkema (Arkema/CNTS-ENSAM-Cnam) for partial support. The authors wish to thank Sylvie Tencé-Girault for the WAXS measurements, analysis and discussion,

David André for the discussion on Hansen's solubility parameters and Stéphane Bizet, Thibaut Bénéthuilière and Xavier Chevalier for fruitful discussions.

References

(1) Roeseler, W. G.; Sarh, B.; Kismarton, M. U. Composite Structures: The First 100 Years; Kyoto, 2007; p 10.

(2) Norkhairunnisa, M.; Chai Hua, T.; Sapuan, S. M.; Ilyas, R. A. Evolution of Aerospace Composite Materials. In *Advanced Composites in Aerospace Engineering Applications*; Springer International Publishing: Cham, 2022; pp 367–385. https://doi.org/10.1007/978-3-030-88192-4_18.

(3) Fried, J. R. *Polymers in Aerospace Applications*; 192; Smithers Rapra Publishing: Shawbury, 2010; p 138. https://chemtec.org/products/978-1-84735-093-0 (accessed 2022-10-26).

(4) Choupin, T.; Fayolle, B.; Régnier, G.; Paris, C.; Cinquin, J.; Brulé, B. Isothermal Crystallization Kinetic Modeling of Poly(Etherketoneketone) (PEKK) Copolymer. *Polymer* **2017**, *111*, 73–82. https://doi.org/10.1016/j.polymer.2017.01.033.

(5) Zhang, L. Hygrothermal Resistance of the Interface in High Performance Polymer Composites. Thesis, University of Toronto, 1998. https://hdl.handle.net/1807/15439.

(6) Pérez-Martín, H.; Mackenzie, P.; Baidak, A.; Ó Brádaigh, C. M.; Ray, D. Crystallinity Studies of PEKK and Carbon Fibre/PEKK Composites: A Review. *Composites, Part B* **2021**, *223*, 109127. https://doi.org/10.1016/j.compositesb.2021.109127.

(7) Vieille, B.; Aucher, J.; Taleb, L. Carbon Fiber Fabric Reinforced PPS Laminates: Influence of Temperature on Mechanical Properties and Behavior. *Adv. Polym. Technol.* **2011**, *30* (2), 80–95. https://doi.org/10.1002/adv.20239.

(8) Merdas, I.; Tcharkhtchi, A.; Thominette, F.; Verdu, J.; Dean, K.; Cook, W. Water Absorption by Uncrosslinked Polymers, Networks and IPNs Having Medium to High Polarity. *Polymer* **2002**, *43* (17), 4619–4625. https://doi.org/10.1016/S0032-3861(02)00267-7.

(9) Cherri, A.; Iliopoulos, I.; Régnier, G.; Brulé, B.; Lé, G.; Tencé-Girault, S. Thermal and Crystallization Properties of the Alternated Tere/Iso PEKK Copolymer: Importance in High-Temperature Laser Sintering. *ACS Appl. Polym. Mater.* **2022**. https://doi.org/10.1021/acsapm.2c00096.

(10) Gardner, K. H.; Hsiao, B. S.; Matheson, R. R.; Wood, B. A. Structure, Crystallization and Morphology of Poly (Aryl Ether Ketone Ketone). *Polymer* **1992**, *33* (12), 2483–2495. https://doi.org/10.1016/0032-3861(92)91128-O.

(11) Arkema. *Kepstan® PEKK Polymer Range*. Arkema. https://www.extrememateials-arkema.com/en/product-families/kepstan-pekk-polymer-range/ (accessed 2022-03-08).

(12) Arkema. *Kepstan 7002*. Arkema. https://www.extrememateials-arkema.com/en/materials-database/products/datasheet/Kepstan%C2%AE%207002 (accessed 2022-10-31).

(13) Victrex. *VICTREX™ PEEK 450G™*. Victrex. https://www.victrex.com/-/media/downloads/datasheets/victrex_tds_450g.pdf (accessed 2022-10-31).

(14) Ma, C.-C. M.; Lee, C.-L.; Chang, M.-J.; Tai, N.-H. Hygrothermal Behavior of Carbon Fiber-Reinforced Poly(Ether Ether Ketone) and Poly(Phenylene Sulfide) Composites. I. *Polym. Compos.* **1992**, *13* (6), 448–453. https://doi.org/10.1002/pc.750130608.

(15) Lucas, J. P.; Zhou, J. The Effects of Sorbed Moisture on Resin-Matrix Composites. *JOM* **1993**, *45* (12), 37–40. https://doi.org/10.1007/BF03222513.

(16) Iqbal, T.; Briscoe, B. J.; Luckham, P. F. Surface Plasticization of Poly(Ether Ether Ketone). *Eur. Polym. J.* **2011**, *47* (12), 2244–2258. https://doi.org/10.1016/j.eurpolymj.2011.09.022.

(17) Arquier, R.; Iliopoulos, I.; Régnier, G.; Miquelard-Garnier, G. Consolidation of Continuous Carbon Fiber-Reinforced PAEK Composites: A Review. *Mater. Today Commun.* **2022**, 104036. https://doi.org/10.1016/j.mtcomm.2022.104036.

(18) Slange, T. K.; Warnet, L. L.; Grouve, W. J. B.; Akkerman, R. Deconsolidation of C/PEEK Blanks: On the Role of Prepreg, Blank Manufacturing Method and Conditioning. *Composites, Part A* **2018**, *113*, 189–199. https://doi.org/10.1016/j.compositesa.2018.06.034.

(19) Yekani Fard, M.; Raji, B.; Pankretz, H. Correlation of Nanoscale Interface Debonding and Multimode Fracture in Polymer Carbon Composites with Long-Term Hygrothermal Effects. *Mech. Mater.* **2020**, *150*, 103601. https://doi.org/10.1016/j.mechmat.2020.103601.

(20) Guo, R.; Xian, G.; Li, C.; Hong, B.; Huang, X.; Xin, M.; Huang, S. Water Uptake and Interfacial Shear Strength of Carbon/Glass Fiber Hybrid Composite Rods under Hygrothermal Environments: Effects of Hybrid Modes. *Polym. Degrad. Stab.* **2021**, *193*, 109723. https://doi.org/10.1016/j.polymdegradstab.2021.109723.

(21) Stober, E. J.; Seferis, J. C.; Keenan, J. D. Characterization and Exposure of Polyetheretherketone (PEEK) to Fluid Environments. *Polymer* **1984**, *25* (12), 1845–1852. https://doi.org/10.1016/0032-3861(84)90260-X.

(22) Courvoisier, E.; Bicaba, Y.; Colin, X. Water Absorption in PEEK and PEI Matrices. Contribution to the Understanding of Water-Polar Group Interactions. *AIP Conf. Proc.* **2016**, *1736* (1), 020036. https://doi.org/10.1063/1.4949611.

(23) Choupin, T.; Fayolle, B.; Régnier, G.; Paris, C.; Cinquin, J.; Brulé, B. A More Reliable DSC-Based Methodology to Study Crystallization Kinetics: Application to Poly(Ether Ketone Ketone) (PEKK) Copolymers. *Polymer* **2018**, *155*, 109–115. https://doi.org/10.1016/j.polymer.2018.08.060.

(24) Mazur, R. L.; Cândido, G. M.; Rezende, M. C.; Botelho, E. C. Accelerated Aging Effects on Carbon Fiber PEKK Composites Manufactured by Hot Compression Molding. *J. Thermoplast. Compos. Mater.* **2016**, *29* (10), 1429–1442. https://doi.org/10.1177/0892705714564283.

(25) Juska, T. Effect of Water Immersion on Fiber/Matrix Adhesion in Thermoplastic Composites. *J. Thermoplast. Compos. Mater.* **1993**, *6* (4), 256–274. https://doi.org/10.1177/089270579300600401.

(26) Tencé-Girault, S.; Quibel, J.; Cherri, A.; Roland, S.; Fayolle, B.; Bizet, S.; Iliopoulos, I. Quantitative Structural Study of Cold-Crystallized PEKK. *ACS Appl. Polym. Mater.* **2021**, *3* (4), 1795–1808. https://doi.org/10.1021/acsapm.0c01380.

(27) Glass, S. V.; Boardman, C. R.; Zelinka, S. L. Short Hold Times in Dynamic Vapor Sorption Measurements Mischaracterize the Equilibrium Moisture Content of Wood. *Wood Sci. Technol.* **2017**, *51* (2), 243–260. https://doi.org/10.1007/s00226-016-0883-4.

(28) Popineau, S.; Rondeau-Mouro, C.; Sulpice-Gaillet, C.; Shanahan, M. Free/Bound Water Absorption in an Epoxy Adhesive. *Polymer* **2005**, *46*, 10733–10740. https://doi.org/10.1016/j.polymer.2005.09.008.

(29) Mensitieri, G.; Apicella, A.; Kenny, J. M.; Nicolais, L. Water Sorption Kinetics in Poly(Aryl Ether Ether Ketone). *J. Appl. Polym. Sci.* **1989**, *37* (2), 381–392. https://doi.org/10.1002/app.1989.070370207.

(30) Humeau, C.; Davies, P.; Jacquemin, F. Moisture Diffusion under Hydrostatic Pressure in Composites. *Mater. Des.* **2016**, *96*, 90–98. https://doi.org/10.1016/j.matdes.2016.02.012.

(31) Davies, P.; Boisseau, A.; Choqueuse, D.; Thiebaud, F.; Perreux, D. Durabilité Des Composites Pour Énergie Marine Renouvelable. In *17èmes Journées Nationales sur les Composites (JNC17)*; Comptes Rendus des JNC 17; Poitiers-Futuroscope, France, 2011; p 34.

(32) Zhan, T.; Sun, F.; Lv, C.; He, Q.; Wang, X.; Xu, K.; Zhang, Y.; Cai, L. Evaluation of Moisture Diffusion in Lignocellulosic Biomass in Steady and Unsteady States by a Dynamic Vapor Sorption Apparatus. *Holzforschung* **2019**, *73* (12), 1113–1119. https://doi.org/10.1515/hf-2019-0063.

(33) Yu, X.; Schmidt, A. R.; Bello-Perez, L. A.; Schmidt, S. J. Determination of the Bulk Moisture Diffusion Coefficient for Corn Starch Using an Automated Water Sorption Instrument. *J. Agric. Food Chem.* **2008**, *56* (1), 50–58. https://doi.org/10.1021/jf071894a.

(34) Bingol, G.; Prakash, B.; Pan, Z. Dynamic Vapor Sorption Isotherms of Medium Grain Rice Varieties. *LWT Food Sci. Technol.* **2012**, *48* (2), 156–163. https://doi.org/10.1016/j.lwt.2012.02.026.

(35) Zhao, X.; Zhang, H.; Li, X.; Fan, W. Extended Dynamic Vapor Sorption of Glutinous Rice Flour Observed in Logarithmic Time Scale and Its Modeling as a Process with Varying Activation Energy. *J. Food Process Eng* **2020**, *43* (12), e13572. https://doi.org/10.1111/jfpe.13572.

(36) Le Gac, P. Y.; Roux, G.; Davies, P.; Fayolle, B.; Verdu, J. Water Clustering in Polychloroprene. *Polymer* **2014**, *55* (12), 2861–2866. https://doi.org/10.1016/j.polymer.2014.04.024.

(37) Burnett, D. J.; Garcia, A. R.; Thielmann, F. Measuring Moisture Sorption and Diffusion Kinetics on Proton Exchange Membranes Using a Gravimetric Vapor Sorption Apparatus. *J. Power Sources* **2006**, *160* (1), 426–430. https://doi.org/10.1016/j.jpowsour.2005.12.096.

(38) Grayson, M. A.; Wolf, C. J. The Solubility and Diffusion of Water in Poly(Aryl-Ether-Ether-Ketone) (PEEK). *J. Polym. Sci., Part B: Polym. Phys.* **1987**, *25* (1), 31–41. https://doi.org/10.1002/polb.1987.090250103.

(39) Merdas, I.; Thominette, F.; Tcharkhtchi, A.; Verdu, J. Factors Governing Water Absorption by Composite Matrices. *Compos. Sci. Technol.* **2002**, *62*, 487–492. https://doi.org/10.1016/S0266-3538(01)00138-5.

(40) Burgess, S. K.; Wenz, G. B.; Kriegel, R. M.; Koros, W. J. Penetrant Transport in Semicrystalline Poly(Ethylene Furanoate). *Polymer* **2016**, *98*, 305–310. https://doi.org/10.1016/j.polymer.2016.06.046.

(41) Krishnaswamy, R. K.; Kalika, D. S. Glass Transition Characteristics of Poly(Aryl Ether Ketone Ketone) and Its Copolymers. *Polymer* **1996**, *37* (10), 1915–1923. https://doi.org/10.1016/0032-3861(96)87309-5.

(42) Wang, Q.; Springer, G. S. Moisture Absorption and Fracture Toughness of PEEK Polymer and Graphite Fiber Reinforced PEEK. *J. Compos. Mater.* **1989**, *23* (5), 434–447. https://doi.org/10.1177/002199838902300501.

(43) Zhang, L. (Alex); Piggott, M. R. Water Absorption and Fiber-Matrix Interface Durability in Carbon-PEEK. *J. Thermoplast. Compos. Mater.* **2000**, *13* (2), 162–172. https://doi.org/10.1177/089270570001300205.

(44) Carter, H. G.; Kibler, K. G. Langmuir-Type Model for Anomalous Moisture Diffusion In Composite Resins. *J. Compos. Mater.* **1978**, *12* (2), 118–131. https://doi.org/10.1177/002199837801200201.

(45) De Nicola, A.; Correa, A.; Milano, G.; La Manna, P.; Musto, P.; Mensitieri, G.; Scherillo, G. Local Structure and Dynamics of Water Absorbed in Poly(Ether Imide): A Hydrogen Bonding Anatomy. *J. Phys. Chem. B* **2017**, *121* (14), 3162–3176. https://doi.org/10.1021/acs.jpcb.7b00992.

(46) Musto, P.; Ragosta, G.; Mensitieri, G. Time-Resolved FTIR/FTNIR Spectroscopy: Powerful Tools to Investigate Diffusion Processes in Polymeric Films and Membranes. *e-Polymers* **2002**, *2* (1). https://doi.org/10.1515/epoly.2002.2.1.220.

(47) van Krevelen, D. W.; Te Nijenhuis, K. Chapter 7 - Cohesive Properties and Solubility. In *Properties of Polymers (Fourth Edition)*; van Krevelen, D. W., Te Nijenhuis, K., Eds.; Elsevier: Amsterdam, 2009; pp 189–227.

(48) Small, P. A. Some Factors Affecting the Solubility of Polymers. *J. Appl. Chem.* **1953**, *3* (2), 71–80. https://doi.org/10.1002/jctb.5010030205.

(49) Fedors, R. F. A Method for Estimating Both the Solubility Parameters and Molar Volumes of Liquids. *Polym. Eng. Sci.* **1974**, *14* (2), 147–154. https://doi.org/10.1002/pen.760140211.

(50) Colin, X. Nonempirical Kinetic Modeling of Non-FIckian Water Absorption Induced by a Chemical Reaction in Epoxy-Amine Networks. In *Solid Mechanics and Its Applications*; Springer, 2018; Vol. 2, pp 1–18.

(51) Hansen, C. M. *Hansen Solubility Parameters: A User's Handbook, Second Edition*, 2nd ed.; CRC Press: Boca Raton, 2007. https://doi.org/10.1201/9781420006834.

(52) Abbott, S.; Hansen, C. M.; Yamamoto, H. *Hansen Solubility Parameters in Practice Complete with EBook, Software and Data*, 4th ed.; CRC Press, Boca Raton FL, 2013.

(53) Horta, B. A. C.; Fuchs, P. F. J.; van Gunsteren, W. F.; Hünenberger, P. H. New Interaction Parameters for Oxygen Compounds in the GROMOS Force Field: Improved Pure-Liquid and Solvation Properties for Alcohols, Ethers, Aldehydes, Ketones, Carboxylic Acids, and Esters. *J. Chem. Theory Comput.* **2011**, *7* (4), 1016–1031. https://doi.org/10.1021/ct1006407.

(54) Gaudichet-Maurin, E.; Thominette, F.; Verdu, J. Water Sorption Characteristics in Moderately Hydrophilic Polymers, Part 1: Effect of Polar Groups Concentration and Temperature in Water Sorption in Aromatic Polysulfones. *J. Appl. Polym. Sci.* **2008**, *109* (5), 3279–3285. https://doi.org/10.1002/app.24873.

(55) Coulson, M.; Quiroga Cortés, L.; Dantras, E.; Lonjon, A.; Lacabanne, C. Dynamic Rheological Behavior of Poly(Ether Ketone Ketone) from Solid State to Melt State. *J. Appl. Polym. Sci.* **2018**, *135* (27), 46456. https://doi.org/10.1002/app.46456.